Construction and Building Materials 242 (2020) 118093

Contents lists available at ScienceDirect

Construction and Building Materials

journal homepage: www.elsevier.com/locate/conbuildmat

Interpretation formulas for in situ characterization of mortar strength

Andrea Benedetti *, Mirco Tarozzi

Department of Civil, Chemical, Environmental and Materials Engineering, University of Bologna, Viale Risorgimento 2, 40136 Bologna, Italy

HIGHLIGHTS

- Mortar mechanical properties are needed for masonry building assessment.
- Non destructive tests should allow for on-site evaluation of mortar properties.
- Mohr-Coulomb plasticity is capable to interpret the mechanics of testing tools.
- Many laboratory investigations show the high effectiveness of interpretation formulas.
- On-site comparison of tools highlights the reliability of a combined investigation.

ARTICLE INFO

Article history:
Received 9 July 2019
Received in revised form 19 November 2019
Accepted 4 January 2020

Keywords:
Mortar
In situ investigation
NDT procedure
Mohr-Coulomb plasticity
Strength evaluation
Ponte Taro Bridge

ABSTRACT

The in situ characterization of mortar mechanical properties is a mandatory activity in every structural assessment of existing monumental buildings. Fine and complex numerical models are meaningless if the material parameters are hypothetical or based on reference values since there exist thousands of mortar compositions and brick types and aging processes do change values in a not easily predictable way.

Therefore direct investigation of the mortar courses is a key ingredient, and this requires specific tools able to deal with thin layers of materials and requirements of conservation.

There are however several ways able to investigate mortars without extracting consistent specimens, and most of them can be interpreted within the common framework of a Mohr-Coulomb plasticity constitutive behavior. Several of these techniques are even capable to discriminate superposed repointing layers of sufficient depth.

In the paper, some versatile and effective mortar investigation techniques are reviewed and the formulas for the strength class definition are presented. Then, the predictive ability of the proposed formulas is checked against large experimental campaigns.

Finally, an interesting investigation on the Ponte Taro bridge in Parma is used in comparing the results of different experimental tools. The data show a general good agreement among the mechanical properties extracted with the proposed procedures.

1. State of the art for in situ mortar investigation techniques

1.1. Introduction

A large part of the world's building heritage is composed of masonry structures with ages spanning the last ten centuries. Although the geometries of the ancient monuments are always complex and the design rules almost unknown, the actual powerfulness of the computer resources allows for a detailed pointwise interpretation of the observed behavior and stress evaluation through numerical models [1]. However, the source of possible deviations from reality is only shifted to the level of the material properties definition and in the constitutive law selection [2]. In fact, many experimental techniques exist for brick, stone and mortar characterization, but they require laboratory specimens of a given shape, which are obviously not easy to obtain from an existing masonry, and sometimes are even impossible to cut off due to the artistic nature of the building [3,4].

In the past, several truly non-destructive testing (NDT) techniques have been proposed [5], which are linked with waves (pressure, electric, magnetic, thermal, etc.) that can explore the material mass. These techniques, however, are in general well correlated with density or elastic modulus, but their connection with material strength is at best very poor. In recent times, even owing to the pressure of earthquake mitigation in

* Corresponding author.
E-mail address: andrea.benedetti@unibo.it (A. Benedetti).

https://doi.org/10.1016/j.conbuildmat.2020.118093
0950-0618/

the Mediterranean area, several investigation techniques have been worked out, that allows in situ mechanical characterization of mortars almost in a non-destructive testing (NDT) set up. All the investigation techniques are based on fundamental mechanical principles and, since mortar is well described by a Mohr-Coulomb constitutive law, for most of them it is possible to elaborate a formula that predicts the mortar mechanical properties from the experimental data.

It is to mention that the strength of the masonry is strictly related to the biaxial strength of both mortar and bricks. For existing historical walls the mortar strength is driving directly the masonry strength. Furthermore, the bonding capacity of mortar is very similar to its tensile capacity and it can be inferred from the mortar strength. Therefore, assessing the on-site mortar properties is mandatory for a careful description of the masonry collapse mechanisms. As will be clear in the following, the proposed investigation techniques are able to detect superposed layers of different mortars coming out from subsequent repointing works of the courses.

1.2. Summary of the most diffused techniques

In what follows several available non-destructive, or moderately destructive (MDT) techniques will be reviewed and discussed. Then, on the basis of a Mohr-Coulomb constitutive law, the connection among the experimental data and the mortar parameters will be established. Finally, a number of comparison trials will be introduced, able to demonstrate the high correlation level of the different experimental techniques.

Almost all the NDT and MDT experimental techniques use simple gears or tools which can produce characteristic stress states in the investigated material. Furthermore, these stress states have always central or polar symmetries, so that the problem can be stated as a two-dimensional problem. Thus, all of those stress states permit a simple description in terms of a σ-τ Mohr-Coulomb constitutive relation in the octahedral plane. Since a Coulomb limit behavior is described by two parameters, at least two distinct points (i.e. two different stress states) would be required for a well-defined solution. This is the case in defining cohesion and friction angle for a Coulomb limit surface [6]. As is well known, the trace of the Mohr-Coulomb limit surface in the octahedral plane is a distorted hexagon, and therefore the compression meridian and the tensile meridian show meaningful differences. Stress states in the octahedral plane can be defined by using the cylindrical coordinates $\{\xi, \rho, \theta\}$, with ξ and ρ proportional to the I_1 and J_2 invariants, and θ the Lode angle [6].

As will be clear in the following analyses, all the stress states generated by the NDT tools used for the mortar characterization, produce octahedral stress states between the tensile and the shear meridian (Fig. 1), i.e. in a side of the hexagon in which the radial measure is almost constant and allows defining the ratio of the tensile to compressive strength of the material in a narrow range. In this zone, the Mohr-Coulomb hexagon is very similar to a Drucker-Prager circle [7], and therefore the friction angle is almost constant.

In fact, in mortars with compressive strength spanning from 0 to 10 MPa, the friction angle varies in a narrow band, and the ratio k_t of the tensile to compressive strength shows values in the range {0.25, 0.35}, very similar to the Poisson Ratio ν, with larger values for weaker mortars [2].

So, basic techniques as indentation, insert extraction, punching failure, splitting failure are conceptually attractive, even if they draw only one experimental value since they can be made so small to adapt to the thin thickness of the mortar courses.

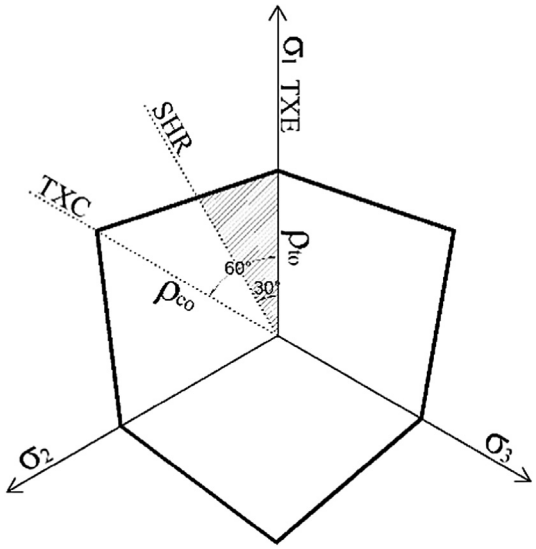

Fig. 1. Trace of the Mohr-Coulomb yield surfaces in the octahedral plane. The grey area indicates the domain of interest in which the results of the proposed NDT tools are included. Modified figure from Chen & Han [6].

The NDT set up which will be presented are:

- Torque penetration test (TPT) or micro vane test,
- Helifix helical fasteners pull out test (HPT).

The MDT set up that will be presented are:

- Splitting test of cores with a rotated mortar layer (SRM),
- Double punch test of mortar layers (DPT).

Other investigation techniques in which is measured the energy consumption needed to damage the material are not considered here. In particular, in the literature, the well-known Gucci drilling penetrometer [8], the pin penetration test [9], and the pointing hardness tester [10] are widely discussed. However, they require an energy conversion into stress states and therefore their precision appears questionable with respect to test types in which the failure force is directly measured.

Felicetti and Gattesco [11] presented an investigation on a pin penetration test derived from timber testing and derived an interpretation formula for the mortar strength based on the penetration depth. Liberatore et al. [12] presented a displacement controlled static penetration test that allows continuous recording of the penetration force. This experimental device is very effective in testing mortar even with several superposed layers, but it is cumbersome and requires significant preparation work before the test.

Regarding tests carried out on cores including mortar layers, it is to say that besides splitting tests intended to define mortar properties, there is the possibility of executing compression tests on the cores by capping them with spreader blocks [13]. Although in this way the compressive strength of the masonry is obtained, the size of those specimens sometimes can be incompatible with the need for conservation of the masonry texture.

1.3. Aim of the study

The on-site detection of mechanical properties of construction materials has attracted a long research interest, due to its importance in safety verification procedures. However, most of the investigation techniques are interpreted in terms of best-fit regression curves, unable to explain the mechanics underneath the test configuration and operation.

In this study, the aim is in filling the gap by using a Mohr-Coulomb constitutive behavior as a general framework for the interpretation of the test results.

The initial variability of the mortar quality from wall to wall and the changes due to partial repointing of the joints are good reasons for the development of effective investigation tools.

The compressive strength of the mortar is extremely important for the evaluation of masonry behavior. Masonry's strength comes out from the interaction of brick and mortar. During the compression, bricks are in a tension–compression state while mortar is in a compression – compression state. Then the masonry strength is defined by the first failing material. Therefore if the mortar is sufficiently strong, the failure will happen by cracking the bricks. Instead, for weak mortar as the one found in historical constructions, the biaxial compressive strength of mortars is the weakest link of the chain, and leads to failure by joint disruption and pulverization.

Furthermore, the elastic modulus of mortar is needed to evaluate the elastic modulus of masonry; since it is not possible to extract the modulus of mortar courses, it is necessary to estimate it as a ratio of the strength, and therefore the strength is necessary once more. Concluding knowing the mortar strength is of very high relevance both in the capacity verification and in the strengthening design of masonry structures.

TPT and HFT are the only tools able to examine mortar in situ and along the depth without extracting any masonry specimen. For that reason, they can play a crucial role in the assessment of historical masonry.

2. Description and mechanical interpretation of the experimental techniques

In what follows, the execution procedures of the four experimental techniques will be illustrated. Starting from the mechanical interpretation and the basic assumption of a Mohr-Coulomb material with a known ratio of tensile to compressive strength, formulas expressing the compressive strength in terms of the measured limit load will be derived.

2.1. Torque penetration test (TPT)

A detailed analysis of the test setup named TPT has been presented in Marastoni et al. [14]. The probe consists of a pin with four small fins and a hexagonal head (Fig. 2). It is inserted in a calibrated hole and turned on its axis by a torque wrench. In this way, a tangential stress is exerted in the mortar surrounding the fins.

The analytical model used for the interpretation of the test results is based on the equivalence of the mechanical work of the wrench and the dissipated fracture energy at the failure surface inside the mortar. By assuming that both the elastic modulus E_m and the fracture energy G_m of mortar are described by a power function of the compressive strength f_{mc}, finally, the functional form relating the specific measured torque to the compressive strength of the mortar is obtained.

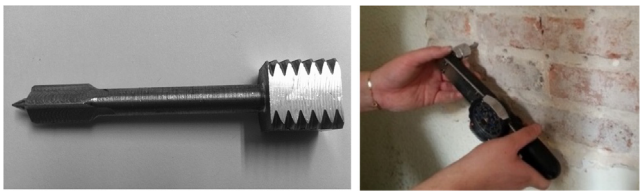

Fig. 2. View of the TPT tool and the torque wrench measurement phase [14].

$$E_m = k_E \cdot \left(\frac{f_{mc}}{f_0}\right)^{\varepsilon},\ G_m = k_G \cdot \left(\frac{f_{mc}}{f_0}\right)^{\gamma} \tag{1}$$

$$f_{mc} = f_0 \cdot \left[\frac{m_v}{2\sqrt{k_E k_G D_e\left(D_e^2 - D_i^2\right)}}\right]^{\frac{2}{\varepsilon+\gamma}} = \left[\frac{m_v}{2\sqrt{55 \cdot D_e\left(D_e^2 - D_i^2\right)}}\right]^{1.274} \tag{2}$$

The constants k_E, k_G, ε, and γ, involved in eq. (1) can be set according to Marastoni et al. [14], while f_0 is a reference compressive strength equal to 1 MPa. In eq. (2) m_v is the torque per unit length of fins, D_i is the diameter of the pilot hole and D_e is the diameter of the cylinder containing the fins.

The prediction capability of this formula has been tested not only with a careful laboratory investigation on mortar blocks and specimen masonry walls but also with reference to a previous experimental campaign carried out by Christiansen [15].

The agreement is very good for all the range of mortar compressive strength (Fig. 3).

2.2. Helical fastener pull out test (HPT)

A very simple test of high robustness is the Helifix pull out test (HPT), in which helical fasteners are pulled by an instrumented device recording the extraction force [16]. The used helices are produced by the Helifix Company UK, under the copyrighted name DryFix.

The fasteners (Fig. 4), normally with an external diameter of 1/4 in. (6.3 mm) or 3/8 in. (9.5 mm) are inserted by screwing them for 30 – 40 mm into the material to be tested in a predrilled hole of diameter containing the solid shaft. For the cited 1/4 in. helix the selected predrilled hole has a diameter of 4.0 mm, and the insertion length is 30 mm.

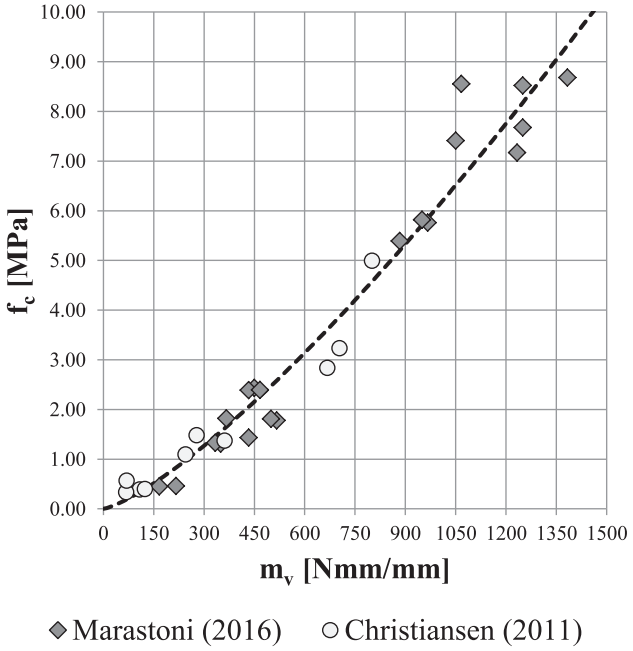

Fig. 3. Comparison of experimental results with the formula of Eq. (2) [14].

Fig. 4. Helical fasteners and Helifix pull out tester.

Some research works were completed in the past [17,18], but the experimental investigations did not lead to a suitable theoretical interpretation of the observed behavior. Moreover, the experimental tests were conducted in mortars and bricks, but only with preliminary conclusions.

Recently, this experimental technique has been applied successfully even to timber elements, showing that HPT is driven by a strong mechanical background [19]. The execution of the HPT is very fast and reliable if care is taken in avoiding contacts with bricks or stones, and internal cavities in the mortar. The test execution has to be smooth and not too fast. The result can be considered representative of the strength if the helix is exiting from the hole filled inside with crushed powder. Different experimenters obtain however very similar results if they take care of the outlined hints.

The use of predrilled holes of different diameters can lead to a shift in the results. The data, however, can be transformed from one setup to the other simply by using the ratio of the mortar volumes extracted by the helices.

In what follows a relevant mechanical interpretation is presented. By supposing that the tool during the extraction does not produce a significant radial compression state in the mortar, the tangential stress τ_H corresponding to the force F pulling out the fastener is derived from the embedment length L and external diameter D_e of the helix:

$$\tau_H = \frac{F}{\pi D_e L} \tag{3}$$

The stress vector, in this case, is straightforward: $\sigma = \{0, 0, 0, \tau_H, 0, 0\}$, and therefore it lays directly in the shear meridian in the Haigh Westergaard space.

The basic relation that connects the friction angle to the ratio of the tensile and the compressive strengths for a Mohr-Coulomb material in an axisymmetric stress distribution is:

$$k_t = \frac{f_t}{f_c} = \frac{1 - \sin\phi}{1 + \sin\phi} \tag{4}$$

Since the predrilled hole reduces considerably the dilatancy effect in the material extracted by the helix during pulling out, the recorded tangential strength corresponds to the Mohr circle centered in the origin of the $\sigma_{OCT} - \tau_{OCT}$ plane:

$$\tau_0 = \frac{f_c f_t}{f_c + f_t} = f_c \frac{k_t}{1 + k_t} \tag{5}$$

The compressive strength of mortar f_{mc} is computed by inverting this formula and introducing the value of τ_H. Although the constant k_t is a function of the friction angle, according to the maximum tensile strength criterion it is very similar to the Poisson ratio. Therefore k_t in lime mortars takes values in the range $0.3 \div 0.4$. Concluding, the compressive strength of mortars can be safely determined with the HFT method by computing $5 \cdot \tau_H$, while for bricks a suitable value is $9 \cdot \tau_H$.

The validation of the proposed formulas is carried on by using a very broad experimentation completed in collaboration by the University of Ferrara and UPC Barcelonatech [20,21].

More precisely five different types of mortar were tested by using EN 1015–11 [3] testing setup (flexural, compression and Brazilian tests on 40·40·160 mm^3 prisms), HPT on mortar courses and DPT on mortar courses. Four of them were prepared in the Laboratory by using commercial products (NHL 3.5 lime, Kerakoll M5 mortar, CL90 aerial lime), while the last one derived from a collection of mortar specimens in the Puig and Cadafalch House in Barcelona [20].

Although some data were not indicated the used helices are of ¼ inch external diameter (6.35 mm), and 1/8 in. internal solid pin (3.15 mm). The helices were inserted for 30 mm in the mortar by using a predrilled hole of 3 or 4 mm. The results of the 3 mm hole can be converted in a 4 mm hole with a factor 0.8 connected with the destroyed volume of mortar in the two cases. The experimental tests were extended for more than 4 months, with a general trend of increasing strength with the age.

Both DPT and HPT were able to detect with a good agreement the strength evolution of the four tested mortar. In the case of the Cadafalch house, although the Normal tests could not be performed, DPT and HPT showed a very good agreement between them.

It is to point out that no interpretation of the observed pull out forces was presented in the cited documents [20,21], while in the present analysis the strength reconstruction has been carried out with reference to the proposed formulations.

Table 1 and Fig. 5 collect the available results of the cited investigations. All the DPT and HPT values were derived with the formulas herein reported.

A further comparison is performed in Fig. 6 with the data of Ferguson & Skandamoorthy [16], and De Vekey & Sassu [18]. As is evident, the theoretical prediction is correcting the bias of the two experimental campaigns and fits very well with the average values of the UPC Barcelonatech investigation.

2.3. Splitting test of cores with rotated mortar layers (SRM)

The mortar properties can be extracted from splitting tests performed on cores including a central mortar layer. An early work is presented in Braga et al. [22], although with the purpose of determining the shear resistance of masonry from this test. Then in Benedetti et al. [23] for the first time, the test was proposed as a way for the statement of the mortar mechanical properties. Finally, in Marastoni et al. [24] and Pelà et al. [25], the test outcomes have been classified and a suitable numerical interpretation was presented.

The SRM test produces a central symmetric failure surface as illustrated in Fig. 7. The confined shear failure of the mortar joints is illustrated in Fig. 8 in which, c and φ are the cohesion and the friction angle of the mortar, f_c is the uniaxial compressive strength, $\{\sigma, \tau\}$ and $\{\Phi \cdot \sigma, \tau\}$ are the stress states in orthogonal and parallel planes to the mortar layer. The ratio of tangential to normal stress is depending on the inclination of the mortar layer with respect to the loading plane. The ratio of the two compressive stresses Φ is depending on the confinement exerted on the mortar by the brick caps, as stated by the Haller – Hilsdorf masonry mechanical model [26].

In this case, the stress tensor is described by the following form:

$$\boldsymbol{\sigma} = \frac{Q}{LD} \begin{bmatrix} -\cos\alpha & \sin\alpha & 0 \\ \sin\alpha & -\Phi_1 \cos\alpha & 0 \\ 0 & 0 & -\Phi_2 \cos\alpha \end{bmatrix} \tag{6}$$

Table 1
Data of the UPC Barcelonatech and Cadafalch House investigations.

Value	UNIT	NHL 3.5	KK. M5	CL 90	NHL-M5	In Situ Clear	In Situ Dark	Average error
f_c	[MPa]	0.91	4.90	0.86	3.13	–	–	
f_{tfl}	[MPa]	0.49	1.80	0.41	1.37	–	–	
k_t	[-]	0.53	0.36	0.48	0.45	–	–	
f_c DPT	[MPa]	0.76	4.45	0.48	3.48	2.291	5.607	
error	[%]	−15.8%	−9.2%	−44.3%	11.2%	–	–	**−14.5%**
f_c HPT	[MPa]	1.32	5.87	–	3.79	1.796	6.212	
error	[%]	46.0%	19.9%	–	20.9%	−21.6%	10.8%	**15.2%**

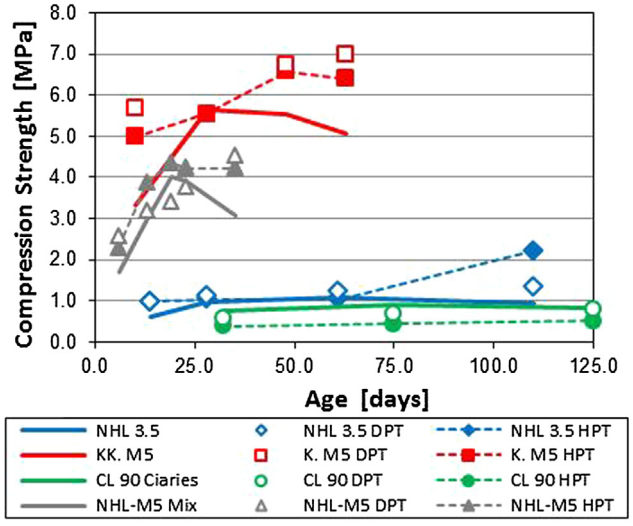

Fig. 5. Aging evolution of mortar strength in the UPC tests [20]

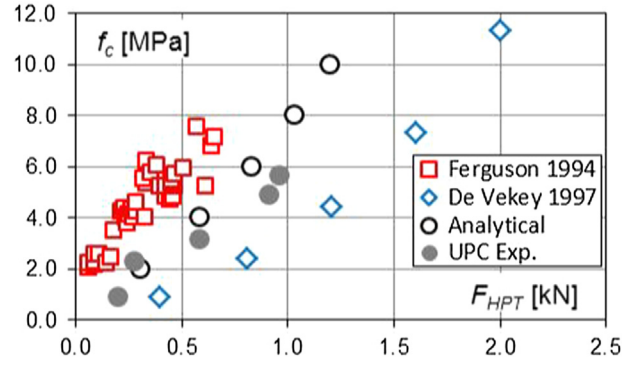

Fig. 6. Comparison of the experimental and analytical results for the HPT device.

With Q the collapse force, L and D the core length and diameter, Φ_1 and Φ_2 the confinement factor of the mortar layer on the two symmetry axes, α the inclination of the mortar layer to the horizontal axis. The analysis of this tensor in the octahedral plane shows that with an inclination pertaining to the set {35°, 40°, 45°, 50°, 55°}, the stress state is laying between the shear and the tensile meridian, as described by the small variation of the normalized radial distance of Fig. 9.

As presented in Fig. 8, the failure is defined by the equation $\overrightarrow{VO} \cdot \sin\varphi = \overrightarrow{OT}$. This limit stress state can be expressed by introducing all the involved quantities in terms of the compressive and tensile strength of the mortar:

$$\frac{f_c f_t}{f_c + f_t} + \frac{1+\Phi}{2}\sigma\frac{f_c - f_t}{f_c + f_t} = \sqrt{\frac{(1-\Phi)^2}{4}\sigma^2 + \tau^2} \tag{7a}$$

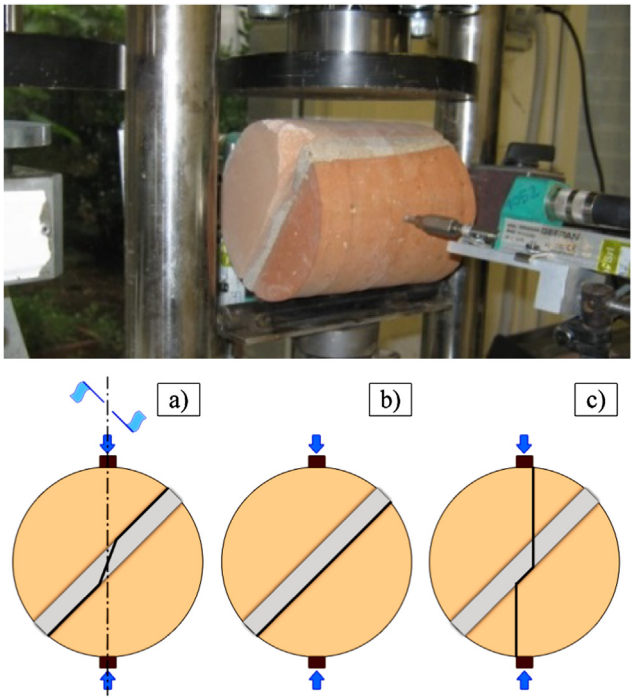

Fig. 7. Brazilian test of cores with rotated mortar layers and possible collapse mechanisms [24].

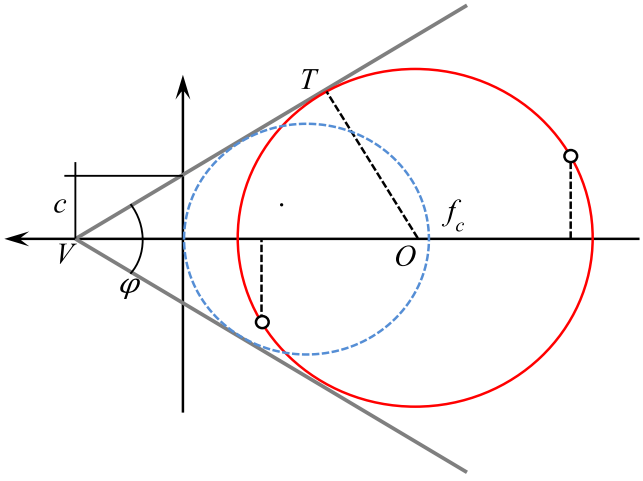

Fig. 8. Representation of the confined shear failure of the mortar joints.

As before, the ratio f_t / f_c is expressed with k_t:

$$f_c \cdot \frac{k_t}{1+k_t} + \frac{1+\Phi}{2}\sigma \cdot \frac{1-k_t}{1+k_t} = \frac{\sigma}{2}\sqrt{(1-\Phi)^2 + 4\tan^2\alpha} \tag{7b}$$

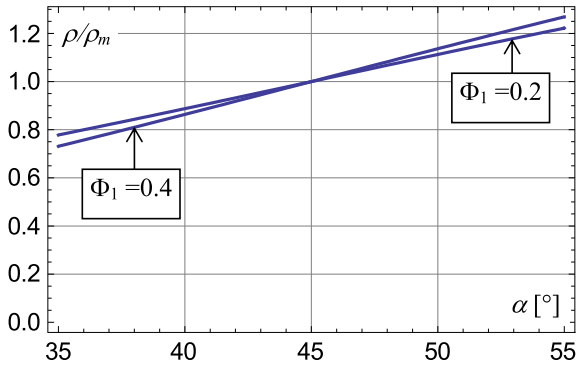

Fig. 9. Variation of the normalized radial distance in the octahedral plane with the SRM specimen inclination.

The ratio of tangential and normal stress is equal to the tangent of the angle α. By collecting the stress σ and expressing it as a function of the failure load Q the following result is obtained:

$$f_c = \frac{Q\cdot\cos\alpha}{L\cdot D}\cdot\frac{1+k_t}{2k_t}\cdot\left[\sqrt{(1-\Phi)^2+4\tan^2\alpha}-\frac{1-k_t}{1+k_t}\cdot(1+\Phi)\right] \quad (8)$$

The confinement depends on the Haller – Hilsdorf parameter Φ describing the horizontal compression generated by the vertical one due to the Poisson ratio mismatch in mortar and bricks [26].

By introducing the brick and mortar Poisson ratios ν_b and ν_m, the modular ratio $\omega = E_m/E_b \ll 1$, and the thickness ratio $\gamma = h_m/h_b \ll 1$, the confinement factor is expressed as in Aprile et al. [26], by equating the brick and mortar stretch in the horizontal direction:

$$\Phi = \frac{\nu_m - \nu_b\cdot\omega}{1-\nu_m+(1-\nu_b)\cdot\omega\cdot\gamma} \approx \nu_m \quad (9)$$

Dealing with historical mortars, k_t is very similar to ν_m with values in the range {0.3; 0.4} due to the principal tension stress failure criterion. Since the best-suited angle α lays in the range {35°; 55°}, also Φ factor has values very similar to ν_m. Therefore a simplified formula can be obtained by directly substituting the cited parameters with ν_m:

$$f_c = \frac{Q\cdot\cos\alpha}{L\cdot D}\cdot\frac{1-\nu_m^2}{2\nu_m}\cdot\left[\sqrt{1+\frac{4\tan^2\alpha}{(1-\nu_m)^2}}-1\right] \quad (10)$$

The predictive capacity of the proposed formulas is checked against the data of two important experimental investigations (Tables 2a and 2b). The UPC Barcelona [24] is a laboratory campaign already discussed. The Forlì campaign is a wide experimental investigation carried out by the Ferrara University at the Forlì City Hall [27].

Table 2a
Data of the experimental campaigns in Barcelona.

Core	Angle [Deg]	D [mm]	L [mm]	P [N]
JC04	45	90	145	10,620
JC11	45	90	145	14,190
JC14	45	90	145	17,870
JC19	45	90	145	14,260
JC02	50	90	145	12,500
JC06	50	90	145	11,530
JC07	50	90	145	10,680
JC09	55	90	145	10,630
JC16	55	90	145	8250
JC05	60	90	145	7120
JC10	60	90	145	9390
JC13	60	90	145	11,320
JC18	60	90	145	10,200
JC21	60	90	145	6690

Table 2b
Data of the experimental campaigns in Forlì City Hall.

Core	Angle [Deg]	D [mm]	L [mm]	Q [N]
D5b	30	110	121	31,110
C2	30	78	146	20,490
B4b	30	110	127	35,020
G3	45	110	140	10,190
C2a	45	110	140	26,530
A3	45	110	140	14,650
F3	45	110	123	22,540
B4b	45	85	110	17,390
C4	45	110	110	9560
G1	45	110	125	22,120
E1	45	44	73	7600
D4b	45	110	129	18,920
C5b	60	110	123	8790
E1	60	110	144	13,160
D1	60	110	138	6890
G2	60	110	138	6280

The data were interpreted with the proposed formulas by using a constant Φ value or a Φ value variable with the inclination of the mortar layer. In Table 3 are summarized the computed values of the mean $E[f_{cm}]$ and the standard deviation $S[f_{cm}]$ of the mortar compressive strength derived from the SRM tests.

The computed average compressive strength was used in order to compare the experimental results with the theoretical interpretation for the investigated rotation angles of the cores subject to the splitting tests (Figs. 10a and 10b).

As is evident from the figures, the simplified formulation is very near to the theoretical one and can be used in deriving the compressive capacity of the mortar even without any confinement pressure estimation. Moreover, the Mohr-Coulomb interpretation is able to explain the effect of the mortar layer inclination in detail.

Table 3
Data of the interpretation of the splitting tests for cores with rotated mortar layer.

Data Set	Φ	k_t	$E[f_{cm}]$	$S[f_{cm}]$	C.O.V.
	[-]	[-]	[MPa]	[MPa]	[%]
UPC	0.35 cos(α)	0.25	2.51	0.44	17.6
	0.25	0.25	2.47	0.44	17.9
Forlì	0.35 cos(α)	0.25	2.87	0.95	33.1
	0.25	0.25	2.91	0.93	32.9

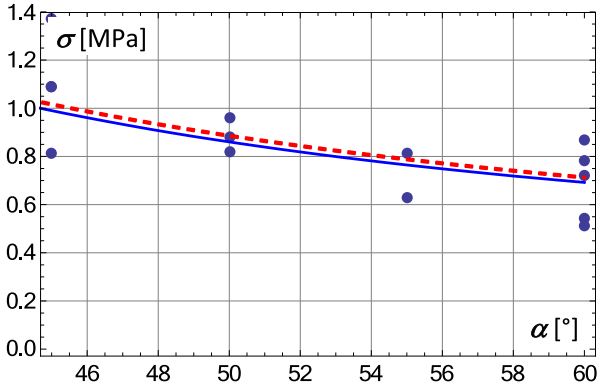

Fig. 10a. Comparison of the UPC data with the analytical model (solid Φ = 0.35 cos α, dashed Φ = 0.25).

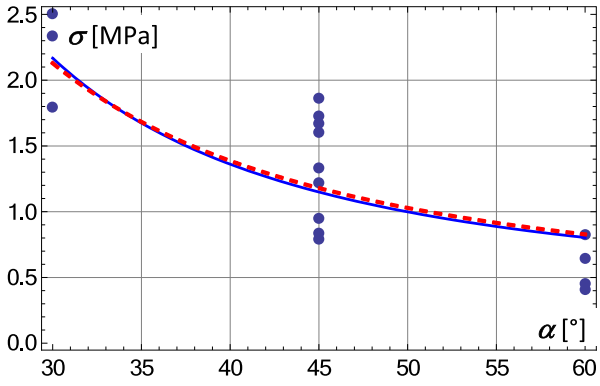

Fig. 10b. Comparison of the Forlì data with the analytical model (solid $\Phi = 0.35 \cos \alpha$, dashed $\Phi = 0.25$).

2.4. Double punch test of mortar layers (DPT)

The punching test of mortar layers illustrated in Fig. 11 is in general performed on specimens extracted from pieces of cores opened after extraction. The use of square plates in the DPT test is very effective if the plates are sufficiently smooth [28]. In Benedetti and Pelà [7] the inverse proportionality of punching pressure with specimen thickness was experimentally shown.

In any case, the result of the test is depending on the friction arising between the mortar layer and the steel punch surfaces. In order of regularizing the contact and reducing the friction, some gypsum or talc powder can be spread between the plate and the punching rods.

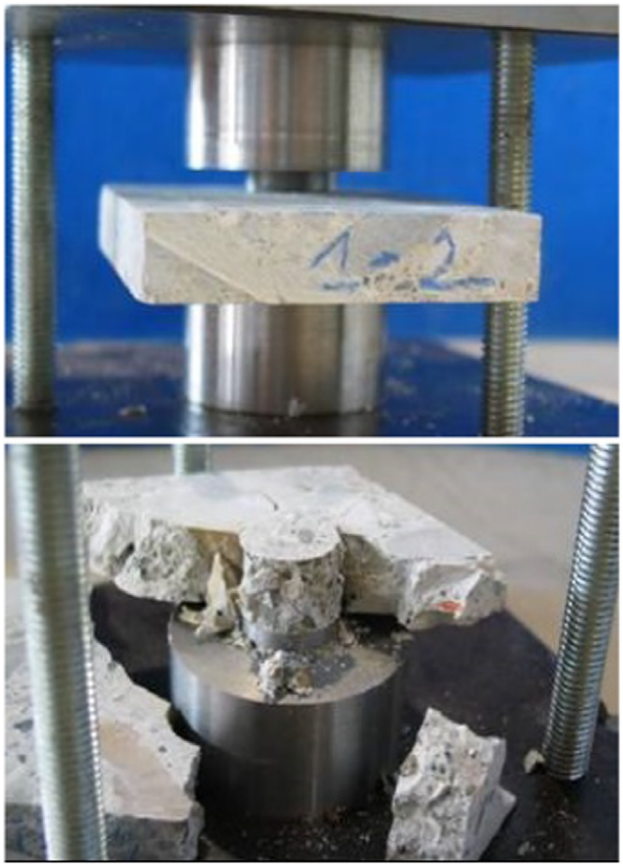

Fig. 11. Double Punch Test for mortar courses. It is easily detectable the formation of a central compressed kernel.

The mechanics of the test (Fig. 12) can be interpreted by considering a confining pressure z exerted by the external tick ring of radius R_e on the internal compressed cylinder of radius R_i and thickness t [6]. A further confining effect is linked with the friction exerted by the steel punch on the mortar surface.

The value of the confining pressure z_F at the collapse of the annular plate is determined by the condition that the stretch of the external ring B has to comply with the expansion of the internal kernel A under the vertical pressure n of the punch. In addition, if the punch is exerting on the mortar a friction radial stress, it can be supposed proportional to the applied pressure and the friction coefficient μ:

$$z_F = \mu n \frac{\pi R_i^2}{2\pi R_i t} = n \cdot \mu\eta \tag{11}$$

η is the shape factor of the inner cylinder that holds $R_i/2t$. The radial stretch of the inner cylinder and the radial expansion of the external ring hold:

$$u_A = \frac{pR_i}{E}\nu - (z + n \cdot \mu\eta)\frac{R_i}{E}(1-\nu),\ u_B = \frac{zR_i}{E}\left(\frac{R_e^2 + R_i^2}{R_e^2 - R_i^2} + \nu\right) \tag{12}$$

By equating the two displacements and posing the radius ratio as $\beta = R_e/R_i$ the mutual confining elastic pressure z_e is evaluated:

$$z_e = \frac{\beta^2 - 1}{2\ \beta^2}[\nu - \mu\eta(1-\nu)]n = \chi_e \cdot n \tag{13}$$

The collapse is occurring mainly by the tensile failure of the external ring. Therefore the Poisson coefficient is not very different from the initial one since the confinement is very low. Namely, for a disk with a length of the outer side equal to two times the diameter of the punches, the elastic interaction formula (13) shows that the confining pressure is of the order of 1/10 of the vertical one.

The limit confining pressure $z_{\lim}$ is the one producing the opening of at least two radial cracks in the external ring. At this moment the confinement is disappearing and the internal compressed cylinder is failing by crushing. The tensile stresses in the external ring are distributed smoothly and attain the maximum value at the two shortest symmetry sections.

Fig. 13 shows the stresses in a 50x50 mm^2 mortar plate acted by a 1 MPa radial pressure (E_m = 1000 MPa, ν_m = 0.25). As is clearly highlighted in the finite element analyses, the external ring failure is occurring with tangential tractions larger than the radial compression. Therefore, once the limit confining pressure $z_{\lim}$ is

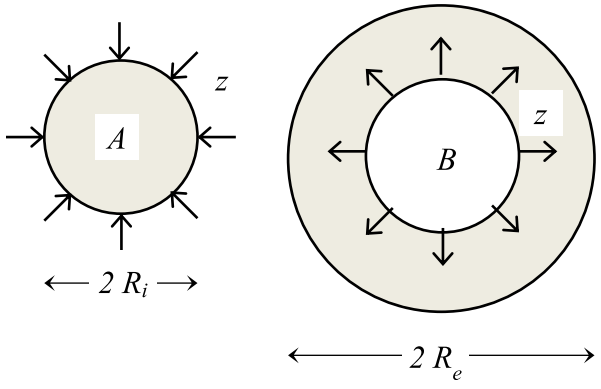

Fig. 12. Schematics of the interaction of the kernel A under the pressure n of the punch, with the surrounding annular plate B producing the mutual radial pressure z.

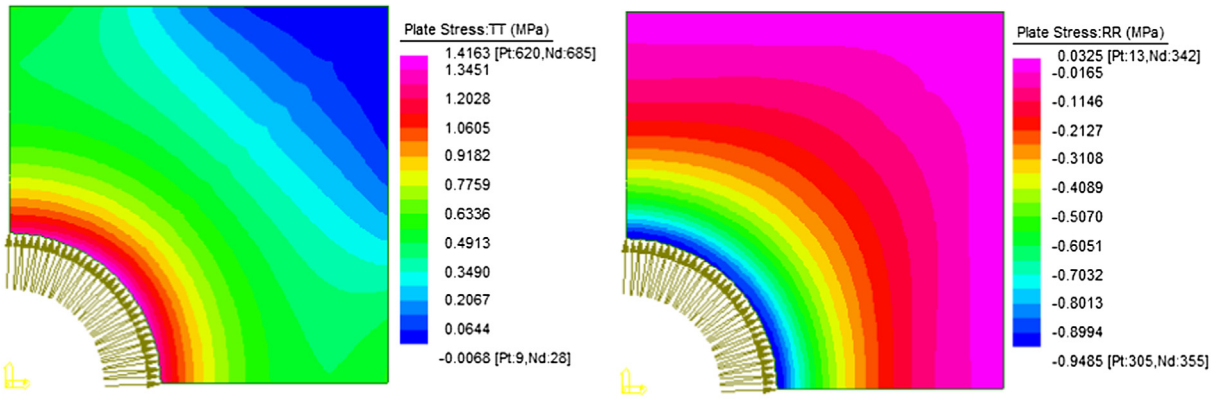

Fig. 13. Tensile stress distribution in the slab surrounding the inner loaded cylinder compressed by a 1 MPa radial mutual pressure.

reached, two radial cracks propagate in the shortest sections outside the compressed area.

By observing that the actual radial stress σ_r (in compression) holds $z_{\lim}$ while the tangential stress σ_t (in tension) holds $z_{\lim}(-\beta^2 + 1)(\beta^2-1)^{-1}$, the failure condition of this section can be easily expressed according to the Mohr-Coulomb biaxial limit:

$$\frac{\sigma_t}{f_t}+\frac{\sigma_r}{f_c}=\frac{z_{\lim}\frac{\beta^2+1}{\beta^2-1}}{f_t}+\frac{z_{\lim}}{f_c}=1 \tag{14}$$

Then, by substituting $f_t = k_t f_c$ in the previous equation (14), the value of the limit confining pressure $z_{\lim}$ can be easily computed as follows:

$$z_{\lim}=f_c\cdot\left(\frac{1}{k_t}\frac{\beta^2+1}{\beta^2-1}+1\right)^{-1} \tag{15}$$

The peak value of the punching force is determined by applying the Mohr-Coulomb criterion at the central cylinder acted on by the vertical pressure and the limit confining pressure occurring at the cracking of the external ring:

$$\left[\frac{c}{\tan\phi}+\frac{n+(z_{\lim}+z_F)}{2}\right]\cdot\sin\phi=\frac{n-(z_{\lim}+z_F)}{2} \tag{16}$$

All the mechanical parameters of the Mohr-Coulomb constitutive relation can be expressed in terms of f_c and k_t. By this way the following relation is obtained:

$$f_c=n-\frac{z_{\lim}+z_F}{k_t} \tag{17}$$

By substituting the previous formulas (11, 15) into the equation (17) the final relation is obtained:

$$f_c=n\cdot(1-\mu\eta)\frac{\beta^2(1+k_t)+(1-k_t)}{\beta^2(2+k_t)-k_t}=n\cdot\chi_p \tag{18}$$

The previous formula allows computing the mortar compressive strength if the k_t coefficient is known and the friction is estimated on the basis of the test setup. As a first approximation, if gypsum powder is introduced between the mortar and the punch, the friction can be disregarded. If the punch is in direct contact with a clean mortar surface, a factor μ = 0.30 can be used, typical of friction forces between rough steel surfaces.

The formula predicts collapse pressures in excess of 20% to 50% of the uniaxial strength as a function of the radius ratio β and the aspect ratio η, as is usually verified in experiments, with larger differences when the friction is not eliminated.

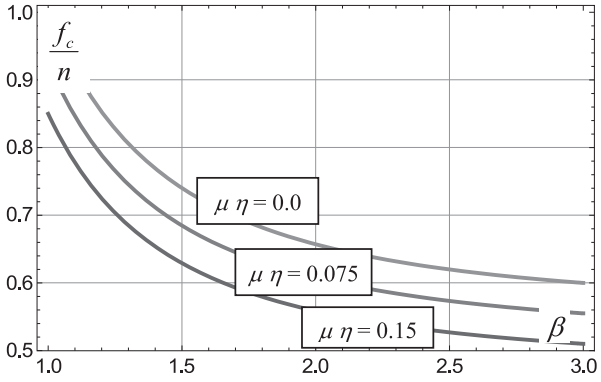

Fig. 14. Strength ratio f_c/n of the specimen as a function of the radius ratio β and the friction coefficient μ multiplied by the aspect ratio η.

Fig. 14 shows the typical trend assumed by the strength ratio f_c/n of the specimen as a function of the radius ratio ρ for three different levels of friction μ.

As a matter of example in Table 4 are reported six punching tests carried out on the mortar used in a wide experimental campaign of masonry wallets [29]. The used MP 910 mortar is characterized by a nominal compressive strength of 10 MPa. The performed DPT tests agree very well with this reference parameter either by using a gypsum powder antifriction layer (case g, μ = 0.0) or simply by punching the layers without any interposed material (case f, μ = 0.3).

The reliability of this experimental set up is even demonstrated in the literature by comparison with many other laboratory tests. For instance, the experimental campaign conducted by Marastoni et al. [24] and Pelà et al. [30] dealt with standard and non-standard tests for mortar characterization and provided DPT results in good agreement with all the other laboratory set up.

3. In situ investigations through combined tests

In what follows the relative predictive capacity of the discussed techniques is outlined with reference to a wide experimental campaign performed on one of the oldest masonry bridges in Italy, namely the Ponte Taro bridge built 1822 by the Duchess Maria Luigia Habsburg Lorena [31] and illustrated in Fig. 15. The extraction of material parameters from old masonry bridges is, in any case, a demanding activity due to the interaction of subsequent weathering and repair phases [32]. Thus the materials of the bridge piers have been characterized by using different NDT tools, including TPT, HFT, SRM. The test concerned both bricks and mortars.

Table 4
Results of the punching tests for the MP 910 mortar.

Element	t	B	σ_p	β	μ	$(1-\mu\cdot\eta)$	χ_p	f_{cm}
	[mm]	[mm]	[MPa]	[-]			[-]	[MPa]
L01-g	9.00	38.00	16.81	1.90	0.0	1.00	0.674	11.33
L01-f	8.00	36.50	22.77	1.83	0.3	0.65	0.445	10.13
L02-g	6.50	39.00	11.81	1.93	0.0	1.00	0.671	7.92
L02-f	5.50	40.00	26.15	2.00	0.3	0.43	0.288	7.53
L03-g	8.00	43.00	14.51	2.13	0.0	1.00	0.651	9.46
L03-f	6.00	41.00	28.54	2.05	0.3	0.47	0.309	8.81

Fig. 15. The Ponte Taro Bridge from the Parma bank.

The performed tests were planned in order to build up a finite element model able to match static and dynamic tests performed on the bridge [31]. Then the model was used in the seismic vulnerability evaluation of the bridge. This demanding task would have not been possible without knowing with high precision the strength distribution of the materials in this two-century old bridge.

The mortar characterization was to some extent more demanding than brick evaluation since, during the bridge life, the external mortar layer has been deteriorated and repointed several times, by using each time a more compact and resistant compound.

Therefore, it is to consider that TPT values, in general, will detect inner weaker mortar while HFT will produce a strength almost linked with exterior mortar. Finally, SRM will detect the average strength of the mortar in each core piece possessing the correct geometry for the test (Figs. 16 and 17).

Although the cited tests suffered the multi-material detection problem previously discussed, the results of the evaluated parameters are in quite good agreement.

Fig. 16. Extraction of specimens from positions 4.

Fig. 17. Cores extracted in positions 4 and 16.

In the following table, the results of the compared investigations are presented. The analysis involved 4 piers (P-01, P-04, P-10, P-16, numbers starting from the Parma side). On each pier, 4 mortar local evaluations were completed, each one composed of three tests of each type (TPT, HFT, SRM).

The reported average values of Table 5 are listed by expressing the tangential stress computed from the peak force recorded

Table 5
Experimental limit shear stress of the Ponte Taro mortar obtained from the three tests.

Test	Position	P-01	P-04	P-10	P-16
		[MPa]	[MPa]	[MPa]	[MPa]
TPT	A	–	6.81	–	–
	B	–	5.15	7.86	–
	C	–	6.16	–	4.98
	D	–	5.59	–	–
HPT	A	–	–	–	–
	B	–	–	1.09	–
	C	–	0.90	–	1.04
	D	–	–	–	–
SRM	A	2.33	1.83	2.31	1.12
	B	–	–	–	–
	C	1.99	1.12	1.66	1.41
	D	–	–	–	–

Table 6
Comparison of the different tools in the prediction of the Ponte Taro mortar mechanical parameters.

test		P-01	P-04	P-10	P-16
SRM	[MPa]	6.64	4.53	5.27	4.72
TPT	[MPa]	–	4.07	5.20	3.25
Error TPT	[%]	–	−10.1%	−1.4%	−31.1%
HPT	[MPa]	–	4.04	4.93	4.67
Error HPT	[%]	–	−10.8%	−6.6%	−0.9%

in the test. As is evident from Table 5, the HPT values are the smallest, while the TPT values are the largest. The different tangential stresses obtained in the three test procedures are depending on the material confinement levels connected with the test procedures. Obviously, the TPT tool produces the highest confinement on the failure surface, and thus results in the highest tangential stress.

However, when the values are transformed into the experimental mortar compressive strength by using the formulas previously discussed, the three procedures converge to the same values since the proposed theories take into consideration the specific confinement ratio of each test set up. The strength values were computed with a Poisson ratio $\nu_m = 0.30$.

The final agreement among the three investigation techniques is noticeable, even if the piers suffered a repeated in time repointing of the deteriorated courses (Table 6). In the error calculations, the SRM values were considered the reference set for the mortar strength.

The relatively large difference of the TPT values are a consequence of the depth at which the tool is fracturing the mortar, since the inner mortar, as explained previously, is certainly weaker than the more recent external one. Concluding, the insight of mortar behavior gained with the combination of different tests permitted to address the differences in the results to the different strengths of the existing mortar layers.

4. Conclusions

The paper presents a compendium of formulas able to interpret a wide variety of experimental set up under the common framework of the Mohr-Coulomb plasticity. It is evident that the on-site characterization of the mortar is a complex task that requires a sound knowledge of the construction history of the monument, mainly from the point of view of the subsequent modification and repair activities.

Since the presented tests involve a different degree of damage to the existing masonry structure, they can comply with different protection requirements for the building. However, since they present a very similar prediction ability, their combination is in principle not necessary, although recommended in order to reduce the variability of the results. Since TPT and HFT are very fast investigation techniques, they can be used even in the mapping of the different mortar and brick types present in a building with a long construction and modification process.

Furthermore, since most of the specimen extraction tools (like coring drills with water cooling, see [13,21]) can damage the material to be tested in the laboratory, the use of laboratory tests alone is not recommended.

The presented experimental data are extracted from a wide set of investigations, which outline most of the problems encountered in the definition of the material properties for old masonry structures. The identification of the problems to be faced when an investigation is to be planned is in itself a valuable tool for experimental researchers.

CRediT authorship contribution statement

Andrea Benedetti: Conceptualization, Methodology, Software, Validation, Writing - original draft, Writing - review & editing, Supervision. **Mirco Tarozzi:** Methodology, Software, Validation, Writing - review & editing.

Declaration of Competing Interest

The authors declare that they have no known competing financial interests or personal relationships that could have appeared to influence the work reported in this paper.

References

[1] P. Roca, M. Cervera, G. Gariup, L. Pelà, Structural analysis of masonry historical constructions. Classical and advanced approaches, Arch. Comput. Methods Eng. 17 (2010) 299–325, https://doi.org/10.1007/s11831-010-9046-1.
[2] Paulo B. Lourenço, Masonry Modeling, in: Michael Beer, Ioannis A. Kougioumtzoglou, Edoardo Patelli, Siu-Kui Au (Eds.), Encyclopedia of Earthquake Engineering, Springer Berlin Heidelberg, Berlin, Heidelberg, 2015, pp. 1419–1431, https://doi.org/10.1007/978-3-642-35344-4_153.
[3] EN 1015-11:2007, 2007. Methods of test for mortar for masonry. Part 11 - Determination of flexural and compressive strength of hardened mortars. CEN, Lausanne, SU.
[4] EN 1015-12:2002, 2002. Methods of test for mortar for masonry. Part 12 - Determination of adhesive strength of hardened rendering and plastering mortars on substrates. CEN, Lausanne, SU.
[5] D.M. McCann, M.C. Forde, Review of NDT methods in the assessment of concrete and masonry structures, NDT&E Int. 34 (2) (2001) 71–84, https://doi.org/10.1016/S0963-8695(00)00032-3.
[6] W.F. Chen, D.J. Han, Plasticity for Structural Engineers, Springer-Verlag New York Inc., USA, 1988.
[7] M. Wojciechowski, A note on the differences between Drucker-Prager and Mohr-Coulomb shear strength criteria, Studia Geotechnica et Mechanica 40 (3) (2018) 163–169, https://doi.org/10.2478/sgem-2018-0016.
[8] N. Gucci, R. Barsotti, A Non-Destructive Technique for the Determination of Mortar Load Capacity in Situ, Mater. Struct. 28 (5) (1995) 276–283, https://doi.org/10.1007/BF02473262.
[9] R. Schmiedmayer, Nondestructive in situ determination of mortar load capacity using a modified Schmidt rebound hammer, in: Proceedings of the 11th IB2MAC Conference. pp. 367-375. Tongij University, Shanghai, China, 14 - 16 October
[10] L.J.A.R. Van Der Klugt, The pointing hardness tester - an instrument to meet a need, Mater. Struct. 24 (6) (1991) 471–476, https://doi.org/10.1007/BF02472020.
[11] R. Felicetti, N. Gattesco, A penetration test to study the mechanical response of mortar in ancient masonry buildings, Mater. Struct. 31 (1998) 350–356, https://doi.org/10.1007/BF02480678.
[12] D. Liberatore, N. Masini, L. Sorrentino, V. Racina, M. Sileo, Shawa O. Al, L. Frezza, Static penetration test for historical masonry mortar, Constr. Build. Mater. 122 (2016) 810–822, https://doi.org/10.1016/j.conbuildmat.2016.07.097.
[13] J. Segura, L. Pelà, P. Roca, A. Cabané, Experimental analysis of the size effect on the compressive behavior of cylindrical samples core-drilled from existing brick masonry, Constr. Build. Mater. 228 (2019) 1–13, https://doi.org/10.1016/j.conbuildmat.2019.116759.
[14] D. Marastoni, A. Benedetti, L. Pelà, G. Pignagnoli, Torque Penetrometric Test for the in-situ characterization of historical mortars: fracture mechanics interpretation and experimental validation, Constr. Build. Mater. 157 (2017) 509–520, https://doi.org/10.1016/j.conbuildmat.2017.09.120.
[15] P.D.V. Christiansen, In Situ Determination of the Compressive Strength of Mortar Joints Using an X-Drill, Masonry Int. (2011) 24.
[16] W.A. Ferguson, J.S. Skandamoorthy, The Screw Pull-out Test for the in-Situ Measurement of the Strength of Masonry Materials, in: Proceedings of the 10th International Brick and Block Masonry Conference. pp. 1257–1266. Calgary, Canada, 1994.
[17] R.C. De Vekey, In-Situ tests for masonry, in: Proceedings of the 09th IB2MAC Conference. pp. 620-627. Berlin, Germany, 13-16 October, 1991.
[18] R.C. De Vekey, M. Sassu, Comparison of non-destructive in-situ mechanical tests on masonry mortars: the PNT-G method and the helix method, in: Proceedings of the 11th IB2MAC Conference. pp. 367-375. Tongij University, Shanghai, China, 14 - 16 October, 1997.
[19] A. Benedetti, M. Tarozzi, Toward a quantitative evaluation of timber strength through on-site tests, in: 7th Int. Conf. on Structural Engineering, Mechanics and Computations. Cape Town (ZA), 2-4 September 2019. doi:10.1201/9780429426506.
[20] E. Regni, Mechanical Characterization of Historical Mortars and Bricks Using Minor Destructive Techniques, Ferrara University Master Thesis (2016). https://www.wisecivil.it/tesi-di-laurea/.

[21] L. Pelà, P. Roca, A. Aprile, Combined in-situ and laboratory minor destructive testing of historical mortars, Int. J. Architectural Heritage 18 (3) (2018) 334–339, https://doi.org/10.1080/15583058.2017.1323247.
[22] F. Braga, M. Dolce, B. Filardi, A. Masi, D. Nigro, A Test Method to Assess the Shear Strength of Existing Masonry Structures - Theoretical Basis and First Experimental Results, in: Proceedings of Int. Workshop Effectiveness of Injection Techniques for Retrofitting of Stone and Brick Masonry Walls in Seismic Areas. pp. 207-227. CNR-GNDT. Milano, Italy, 1992.
[23] A. Benedetti, L. Pelà, A. Aprile, Masonry properties determination via splitting tests on cores with a rotated mortar layer, in: B. Sinha, L. Tanaçan (Eds.), Masonry properties determination via splitting tests on cores with a rotated mortar layer, Istanbul Technical University, Turkey, 2008, pp. 647–655.
[24] D. Marastoni, L. Pelà, A. Benedetti, P. Roca, Combining Brazilian tests on masonry cores and double punch tests for the mechanical characterization of historical mortars, Constr. Build. Mater. 112 (2016) 112–127, https://doi.org/10.1016/j.conbuildmat.2017.09.120.
[25] L. Pelà, P. Roca, A. Benedetti, Mechanical Characterization of Historical Masonry by Core Drilling and Testing of Cylindrical Samples, Int. Journal of Architectural Heritage 10 (2016) 360–374, https://doi.org/10.1080/15583058.2015.1077906.
[26] A. Aprile, A. Benedetti, F. Grassucci, Assessment of Cracking and Collapse for old Brick Masonry Columns, J. Struct. Eng. 127 (2001) 1427–1435, https://doi.org/10.1061/(ASCE)0733-9445(2001) 127:12(1427).
[27] DICAM, Relazione tecnica d'interpretazione dei materiali presenti nel Palazzo Comunale di Forlì (in italian). LISG Laboratory report, DICAM Department, University of Bologna, Italy, 2010.
[28] J. Henzel, S. Karl, Determination of Strength of Mortar in the Joints of Masonry by Compression Tests on Small Specimens, Darmstadt Concrete 2 (1987) 123–136.
[29] A. Benedetti, In Plane Behaviour of Masonry Walls Reinforced with Mortar Coatings and Fibre Meshes, Int. Journal of Architectural Heritage (2019) 1–13, https://doi.org/10.1080/15583058.2019.1618972.
[30] L. Pelà, K. Kasioumi, P. Roca, Experimental evaluation of the shear strength of aerial lime mortar brickwork by standard tests on triplets and non-standard tests on core samples, Eng. Struct. 136 (1) (2017) 441–453, https://doi.org/10.1016/j.engstruct.2017.01.028.
[31] A. Benedetti, C. Colla, G. Pignagnoli, M. Tarozzi, Static and Dynamic Investigation of the Taro Masonry Bridge in Parma, Italy. Proceedings of the SAHC 2018. pp. 2264-2272. RILEM Bookseries, vol.18, 2019.
[32] A. Brencich, D. Sabia, Experimental identification of a multi-span masonry bridge: The Tanaro Bridge, Constr. Build. Mater. 22 (2008) 2087–2099, https://doi.org/10.1016/j.conbuildmat.2007.07.031.